

Waves in a harbour with partially reflecting boundaries

Michael Isaacson and Shiqin Qu

*Department of Civil Engineering, University of British Columbia, Vancouver, B.C. V6T 1W5
(Canada)*

(Received May 14, 1989; revised and accepted November 21, 1989)

ABSTRACT

Isaacson, M. and Qu, S., 1990. Waves in a harbour with partially reflecting boundaries. *Coastal Eng.*, 14: 193–214.

The present paper describes a method based on linear diffraction theory for predicting the wave field in a harbour containing partially reflecting boundaries. The method utilizes a point source representation of the harbour boundaries and a matching boundary which separates regions interior and exterior to the harbour, and involves the application of a partial reflection boundary condition. Numerical results are presented for the wave field within a rectangular harbour with a pair of symmetrical breakwaters, for cases of fully absorbing, fully reflecting, and partially reflecting boundaries. The method appears to be able to account adequately for the effects of wave diffraction and partial reflections, and to predict the wave field realistically.

INTRODUCTION

The degree of protection provided to vessels within a harbour is a primary consideration in harbour design and consequently improved predictions of wave conditions within a harbour are of considerable importance. The calculation of short wave diffraction in harbours generally ignores wave reflections off the interior boundaries of the harbour. In particular, closed-form solutions for a semi-infinite straight breakwater, and for a breakwater gap between a pair of colinear straight semi-infinite breakwaters have been known for some time and are widely used in marina design (e.g. Shore Protection Manual, 1984).

On the other hand, long wave resonance in harbours has generally been treated by considering all harbour boundaries as impermeable so that a full reflection boundary condition may be applied. Hwang and Tuck (1970) have treated this problem for the case of a harbour of arbitrary shape by the use of a boundary integral method which involves the distribution of wave sources along the harbour boundary. Chen and Mei (1974) treated such problems

using a hybrid element method in which a finite-element solution in the interior region of the harbour is matched to an analytical solution for the exterior region. The special case of resonance in a rectangular harbor has been described by Miles and Munk (1961), Garrett (1970) and Mei (1983).

For the case of short wave propagation, neither of these approaches, corresponding either to complete reflection or to zero reflection at the harbour boundaries is really appropriate since in practice partial reflection at the boundaries within a harbour invariably occurs. The corresponding extension may be made by introducing a partial reflection condition along the harbour boundaries as indicated by Berkhoff (1976). Chen (1986) introduced such a refinement, together with one accounting for bottom friction, to a hybrid element model of wave behaviour within a harbour, and applied this to study the influence of boundary absorption and bottom friction on long wave resonance in a rectangular harbour. An alternative refinement treated by some

NOTATION

A	$-igH/2\omega$
d	still water depth
f	source strength
G	Greens function
g	gravitational constant
H	wave height
$H_m^{(1)}$	Hankel function of the first kind and order m
i	$=\sqrt{-1}$
K_r	reflection coefficient
k	wave number
N	number of segments
n	distance normal to boundary, directed into the fluid region
r	distance between points x and ξ
S	harbour boundary (see Fig. 1)
T	wave period
t	time
$x=(x,y)$	horizontal coordinates of general point
z	vertical coordinate measured upwards from the still water level
α	complex transmission coefficient
β	reflection phase angle
γ	incident wave direction relative to normal at the boundary
Γ	matching boundary (see Fig. 1)
AS	segment length
η	free surface elevation
θ	wave direction relative to x -axis (see Fig. 1)
$\xi=(\xi,\eta)$	horizontal coordinates of wave source on the boundary Γ or S
Φ	velocity potential
ϕ	velocity potential function (see Eq. 4)
ω	angular wave frequency
χ	angle of the boundary normal relative to the x -axis

authors takes account of variable depth by including the effects of combined wave refraction and diffraction.

The present paper attempts to provide a general solution of wave behaviour in a harbour of arbitrary shape and constant depth, based on the approach indicated by Berkhoff (1976) and taking account of partial reflections. Results of a corresponding numerical model are presented for the fundamental case of a wave train incident on a rectangular harbour contained within a symmetrical pair of breakwaters. The harbour boundaries are considered to have varying degrees of reflection, including the limiting cases of perfect reflection and absorption. The results of the model are described by plots of surface elevation, corresponding to an instantaneous view of the wave field, as well as contours of wave height and wave phase.

THEORETICAL FORMULATION

Governing equations

A numerical approach to predicting the wave field within a harbour with partially reflecting boundaries was indicated by Berkhoff (1976) and the application of such a method to a harbour of arbitrary configuration is considered here.

The general situation being investigated is indicated in Fig. 1, with wave motion at a single frequency only being considered. A Cartesian coordinate

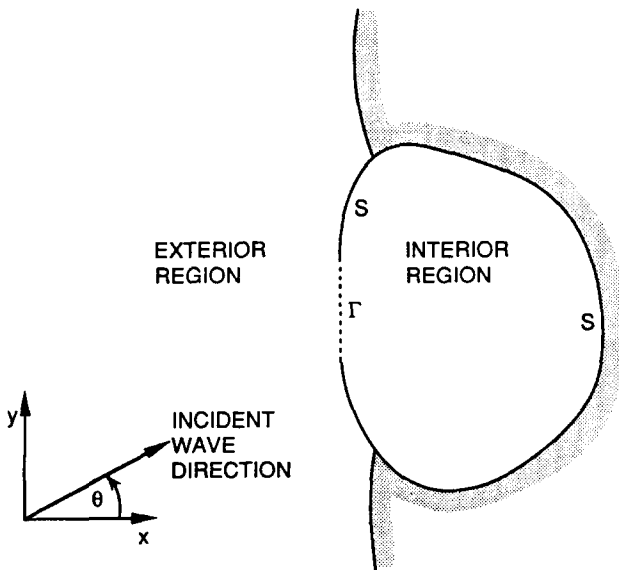


Fig. 1. Definition sketch of the general diffraction problem.

system is defined with x and y measured horizontally and z measured vertically upwards from the still water level. In the usual manner the fluid is assumed incompressible and inviscid and the flow irrotational so that the flow may be described by a velocity potential Φ which satisfies the Laplace equation within the fluid region. Thus the effects of fluid viscosity are confined to energy absorption and resulting partial reflection along the harbour boundaries. The wave height is assumed sufficiently small for nonlinear terms to be omitted so that linear wave theory is applicable. The seabed and two free-surface boundary conditions are given as:

$$\frac{\partial \Phi}{\partial z} = 0 \quad \text{at } z = -d \quad (1)$$

$$\frac{\partial^2 \Phi}{\partial t^2} + g \frac{\partial \Phi}{\partial z} = 0 \quad \text{at } z = 0 \quad (2)$$

$$\eta = -\frac{1}{g} \left(\frac{\partial \Phi}{\partial t} \right)_{z=0} \quad (3)$$

Here η is the free surface elevation, g is the gravitational constant, d is the still water depth and t is time.

Provided that all barriers are considered vertical and to extend from the seabed (or deep water) up to the free surface, the velocity potential Φ may be considered to have the following form:

$$\Phi(\mathbf{x}, z, t) = A\phi(\mathbf{x}) \frac{\cosh[k(z+d)]}{\cosh(kd)} \exp(-i\omega t) \quad (4)$$

where $\phi(\mathbf{x})$ denotes a two-dimensional potential function which is to be determined, and \mathbf{x} represents a general point (x, y) in the horizontal plane. (The real parts of this and subsequent complex expressions are understood.) Also $A = -igH_0/2\omega$, $i = \sqrt{-1}$, H_0 is the incident wave height, k is the wave number, and ω is the angular frequency which is related to the wave number by the linear dispersion relation:

$$\omega^2 = gk \tanh(kd) \quad (5)$$

The free surface elevation corresponding to Eq. 4 is given as:

$$\eta(\mathbf{x}, t) = \frac{H_0}{2} \phi(\mathbf{x}) \exp(-i\omega t) \quad (6)$$

Equation 4 ensures that the seabed and free-surface boundary conditions are satisfied. Since the velocity potential Φ satisfies the Laplace equation, the potential function ϕ itself must satisfy the Helmholtz equation within the fluid region:

$$\frac{\partial^2 \phi}{\partial x^2} + \frac{\partial^2 \phi}{\partial y^2} + k^2 \phi = 0 \tag{7}$$

It is convenient to define an exterior region and an interior region as indicated in Fig. 1, with the boundary between the two areas denoted by Γ . The choice of Γ is somewhat arbitrary, and in certain situations, such as a marina with a single breakwater, such a representation is inappropriate, corresponding to a limitation of the method. Both the interior and exterior regions are assumed to have the same constant water depth and therefore the same wave number k . In the exterior region, the potential ϕ is expressed as a superposition of a known incident wave potential ϕ_w and a scattered wave potential $\phi_s^{(e)}$. The scattered potential is assumed to be due only to the presence of the harbour and thus to emanate from the boundary Γ . That is, in the exterior region, reflections of the incident wave from the breakwater and the shoreline are neglected with respect to their influence on the interior flow field, so that the representation of the exterior flow field itself may not be completely realistic. In the interior region, the potential function ϕ is not separated in this way and is denoted as $\phi_s^{(i)}$. Thus:

$$\phi = \begin{cases} \phi_w + \phi_s^{(e)} & \text{in the exterior region} \\ \phi_s^{(i)} & \text{in the interior region} \end{cases} \tag{8}$$

The incident wave potential ϕ_w is known and may be expressed as:

$$\phi_w(\mathbf{x}) = \exp[i(kx \cos \theta + ky \sin \theta)] \tag{9}$$

where θ is the incident wave direction measured clockwise from the x -axis.

Along the boundary Γ matching conditions relating the flows in the interior and exterior regions may be imposed. Continuity of the free surface elevation and velocity normal to the boundary require that the potential ϕ and its normal derivative $\partial\phi/\partial n$ are continuous. These conditions are respectively:

$$\phi_s^{(i)} = \phi_w + \phi_s^{(e)} \quad \text{on } \Gamma \tag{10}$$

$$\frac{\partial \phi_s^{(i)}}{\partial n} = \frac{\partial \phi_w}{\partial n} + \frac{\partial \phi_s^{(e)}}{\partial n} \quad \text{on } \Gamma \tag{11}$$

In addition, $\phi_s^{(e)}$ is subject to a radiation condition in the far field, and $\phi_s^{(i)}$ is subject to a boundary condition along the harbour boundaries. The radiation condition is:

$$\text{Lim}_{r \rightarrow \infty} \sqrt{r} \left(\frac{\partial \phi_s^{(e)}}{\partial r} - ik \phi_s^{(e)} \right) = 0 \tag{12}$$

where r is distance measured away from the harbour. The boundary condition

along the harbour boundary should take account of partial reflections and is now considered.

Partial reflection boundary condition

A boundary condition corresponding to partial reflection may be introduced in the manner proposed by Berkhoff (1976). Reflecting boundaries are not always vertical nor are fully reflecting. In order to treat these boundaries in the present model, they are schematized as vertical, and partial reflection is introduced into the model by using a mixed boundary condition instead of the full reflection condition. This is:

$$\frac{\partial \phi}{\partial n} + \alpha k \phi = 0 \quad (13)$$

in which n is distance into the fluid region measured normal to the boundary and $\alpha (= \alpha_1 + i\alpha_2)$ is a complex transmission coefficient. This coefficient may be interpreted in a number of ways, as indicated by Berkhoff (1976) and summarized by Isaacson and Qu (1989). These relate to:

- (a) its relation to the rate of transfer of energy at the boundary;
- (b) its relation to the height and phase of the wave field at the boundary;
- and
- (c) its relation to the conventional reflection coefficient.

The transmission coefficient α may be related to the reflection coefficient K_r which is commonly used and which is defined as the ratio of a reflected wave height to an incident wave height. This definition is really only useful in the particular case of reflection of a long-crested plane wave against a long wall, assuming that partial reflection has no influence upon the form of the reflected wave. In such a case it is possible to relate the transmission coefficient $\alpha (= \alpha_1 + i\alpha_2)$ to the conventional reflection coefficient K_r and a phase shift β associated with the reflection, and the angle the incident wave train makes with the wall.

Assuming that a wave train undergoes oblique partial reflection from a vertical wall located at $x=0$, such that the incident wave direction makes an angle γ with the normal to the wall, the total potential of the combined wave field corresponds to a three-dimensional wave pattern and may be written as the sum of the incident and reflected wave potentials:

$$\begin{aligned} \phi = & A \{ \exp [ik(x \cos \gamma + y \sin \gamma)] \\ & + K_r \exp [-ik(x \cos \gamma - y \sin \gamma) + i\beta] \} \end{aligned} \quad (14)$$

Substituting Eq. 14 into Eq. 13 the transmission coefficient α is given as:

$$\left. \begin{aligned} \alpha_1 &= \frac{2K_r \sin \beta \cos \gamma}{1 + K_r^2 + 2K_r \cos \beta} \\ \alpha_2 &= \frac{(1 - K_r^2) \cos \gamma}{1 + K_r^2 + 2K_r \cos \beta} \end{aligned} \right\} \quad (15)$$

Equation 15 shows how the transmission coefficient depends on the conventional reflection coefficient K_r , the reflection phase angle β and the incident wave direction γ . This indicates that for normally incident waves ($\gamma=0^\circ$) the special cases of full reflection with $K_r=1$ and $\beta=0^\circ$ and full absorption with $K_r=0$ and $\beta=0^\circ$ correspond to $\alpha=0$ and i , respectively.

Greens function representation

The boundary value problem which has been specified is solved by expressing the scattered potential $\phi_s^{(e)}$ in the exterior region as due to a distribution of point wave sources along the matching boundary Γ , and the scattered potential $\phi_s^{(i)}$ in the interior region as due to a distribution of point wave sources along the matching boundary Γ and along the remaining harbour boundaries, denoted S as indicated in Fig. 1. Thus:

$$\phi_s^{(e)}(\mathbf{x}) = \frac{1}{4\pi} \int_{\Gamma} f^{(e)}(\xi) G(\mathbf{x}; \xi) dS \quad (16)$$

$$\phi_s^{(i)}(\mathbf{x}) = \frac{1}{4\pi} \int_{S+\Gamma} f^{(i)}(\xi) G(\mathbf{x}; \xi) dS \quad (17)$$

where $f^{(e)}(\xi)$ and $f^{(i)}(\xi)$ represent the source strength distribution functions for the exterior and interior potentials, respectively, $G(\mathbf{x}; \xi)$ is a Greens function for the general point $\mathbf{x} = (x, y)$ due to a point wave source located at the point $\xi = (\xi, \eta)$ on Γ or S , and dS denotes a differential length along Γ or S . The Greens function represents the potential at a general point \mathbf{x} due to a point wave source of unit strength at point ξ and corresponds to a fundamental solution to the Helmholtz equation which satisfies the radiation condition. It may be expressed as:

$$G(\mathbf{x}; \xi) = i\pi H_0^{(1)}(kr) \quad (18)$$

where $H_0^{(1)}$ is the Hankel function of the first kind and zero-th order, and r is the distance between \mathbf{x} and ξ :

$$r = \sqrt{(x - \xi)^2 + (y - \eta)^2} \quad (19)$$

The boundary conditions along Γ given by Eqs. 10 and 11 give rise to the following pair of integral equations for $f^{(i)}$ and $f^{(e)}$:

$$\frac{1}{4\pi} \int_{S+\Gamma} f^{(i)}(\xi) G(\mathbf{x};\xi) dS - \frac{1}{4\pi} \int_{\Gamma} f^{(e)}(\xi) G(\mathbf{x};\xi) dS = \phi_w(\mathbf{x}) \quad \text{for } \mathbf{x} \text{ on } \Gamma \quad (20)$$

$$-\frac{1}{2}f^{(i)}(\mathbf{x}) + \frac{1}{4\pi} \int_{S+\Gamma} f^{(i)}(\xi) \frac{\partial G}{\partial n}(\mathbf{x};\xi) dS + \frac{1}{2}f^{(e)}(\mathbf{x}) - \frac{1}{4\pi} \int_{\Gamma} f^{(e)}(\xi) \frac{\partial G}{\partial n}(\mathbf{x};\xi) dS = \frac{\partial \phi_w}{\partial n}(\mathbf{x}) \quad \text{for } \mathbf{x} \text{ on } \Gamma \quad (21)$$

In addition, the boundary condition along S for the general case of partial reflection given by Eq. 13 gives rise to an integral equation:

$$-\frac{1}{2}f^{(i)}(\mathbf{x}) + \frac{1}{4\pi} \int_{S+\Gamma} f^{(i)}(\xi) \frac{\partial G}{\partial n}(\mathbf{x};\xi) dS + \alpha(\mathbf{x}) \frac{k}{4\pi} \int_{S+\Gamma} f^{(i)}(\xi) G(\mathbf{x};\xi) dS = 0 \quad \text{for } \mathbf{x} \text{ on } S \quad (22)$$

In Eqs. 20, 21 and 22, \mathbf{x} is the point on Γ or S at which the boundary condition is applied, and n is distance in a direction normal to Γ or S at \mathbf{x} . In the case of a fully reflecting portion of a boundary, $\alpha=0$ so that the second integral in Eq. 22 is then absent. In the case of a fully absorbing portion of a boundary, $\alpha=i$. Bearing in mind that r in Eq. 12 and n in Eq. 13 are in opposite directions, it is seen that the radiation condition given in Eq. 12 may then instead be satisfied. Because the Greens function chosen satisfies this condition, this portion of the boundary can then simply be omitted from Eq. 22.

In evaluating the integrals in Eqs. 21 and 22, the derivative of the Greens function $\partial G/\partial n$ is required. This may be expressed as:

$$\frac{\partial G}{\partial n} = -i\pi k H_1^{(1)}(kr) \cos \delta \quad (23)$$

where $H_1^{(1)}$ is the Hankel function of first kind and order one, and:

$$\cos \delta = \frac{n_x(x-\xi) + n_y(y-\eta)}{r} \quad (24)$$

Here n_x and n_y are the direction cosines of the normal vector \mathbf{n} with respect to the x and y directions, respectively.

Numerical approximation

In a numerical solution to the formulation given above, Eqs. 20, 21 and 22 are solved by a numerical procedure in which the horizontal contour $S+\Gamma$ is

discretized into N_S short straight segments along S and N_T segments along Γ , and the source strength is assumed constant over each segment, and denoted by $f_j^{(i)}$ for the j th segment. Using this discretization, Eqs. 20, 21 and 22 are satisfied at the centre of each source segment and are thereby reduced to three sets of linear equations for the unknown source strengths at the centre of each segment. These correspond, respectively, to N_S , N_T and N_T equations for the $N_S + N_T$ values of $f_j^{(i)}$ and the N_T values of $f_j^{(e)}$ which are required. These may be combined into a single set of $N = N_S + 2N_T$ linear equations for all the source strengths:

$$\sum_{j=1}^N A_{ij} \lambda_j = b_i \quad \text{for } i = 1, \dots, N \tag{25}$$

where:

$$\lambda_j = \begin{cases} f_j^{(i)} & \text{for } j = 1, \dots, N_1 \\ f_j^{(e)} & \text{for } j = N_1 + 1, \dots, N \end{cases} \tag{26}$$

$$b_i = \begin{cases} 0 & \text{for } i = 1, \dots, N_S \\ 2\phi_w & \text{for } i = N_S + 1, \dots, N_1 \\ \frac{2\partial\phi_w}{\partial n} & \text{for } i = N_1 + 1, \dots, N \end{cases} \tag{27}$$

$$A_{ij} = \begin{cases} B_{ij} & \text{for } i = 1, \dots, N_S; j = 1, \dots, N_1 \\ 0 & \text{for } i = 1, \dots, N_S; j = N_1 + 1, \dots, N \\ \pm \frac{1}{2\pi} G_{ij} \Delta S_j & \text{for } i = N_S + 1, \dots, N_1 \\ \pm \frac{1}{2\pi} \left[\left(\frac{\partial G}{\partial n} \right)_{ij} \Delta S_j - \delta_{ij} \right] & \text{for } i = N_1 + 1, \dots, N \end{cases} \tag{28}$$

Where alternative signs are given, the positive sign applies when $j = 1, \dots, N_1$ and the negative sign when $j = N_1 + 1, \dots, N$. In the above $N_1 = N_S + N_T$ and G_{ij} and $(\partial G / \partial n)_{ij}$ denote, respectively, G and $\partial G / \partial n$ with argument $(\mathbf{x}_i; \boldsymbol{\xi}_j)$. Also:

$$B_{ij} = -\delta_{ij} + \frac{1}{2\pi} \left[\frac{\partial G}{\partial n} + k\alpha(\mathbf{x}_i) G \right] \Delta S_j \tag{29}$$

δ_{ij} is the Kronecker delta and ΔS_j is the length of the j th segment. For $i \neq j$, B_{ij} is evaluated by assuming $\partial G / \partial n$ and G to be constant over the segment length. However, when $i = j$ a singularity arises so that an integration over the segment is used in place of the mid-point approximation. Bearing this in mind, a suitable approximation for B_{ij} is given as:

$$B_{ij} = \begin{cases} \frac{\Delta S_j}{2\pi} \left[\frac{\partial G}{\partial n}(\mathbf{x}_i; \boldsymbol{\xi}_j) + k\alpha(\mathbf{x}_i) G(\mathbf{x}_i; \boldsymbol{\xi}_j) \right] & \text{for } i \neq j \\ -1 + \frac{\Delta S_i}{\pi} k\alpha(\mathbf{x}_i) \left[\ln\left(\frac{\Delta S_i}{2}\right) - 1 \right] & \text{for } i = j \end{cases} \quad (30)$$

Now that the coefficients A_{ij} are known, the sources strengths f_j may be obtained by solving Eq. 25, and the potential functions $\phi_s^{(e)}(\mathbf{x})$ and $\phi_s^{(i)}(\mathbf{x})$ at a point \mathbf{x} within the interior and exterior regions in turn may then be obtained by discretized versions of Eqs. 16 and 17:

$$\phi_s^{(i)}(\mathbf{x}) = \frac{1}{4\pi} \sum_{j=1}^N f_j^{(i)} G(\mathbf{x}; \boldsymbol{\xi}_j) \Delta S_j \quad (31)$$

$$\phi_s^{(e)}(\mathbf{x}) = \frac{1}{4\pi} \sum_{j=1}^N f_j^{(e)} G(\mathbf{x}; \boldsymbol{\xi}_j) \Delta S_j \quad (32)$$

Description of flow field

Once the potentials $\phi_s^{(e)}$ and $\phi_s^{(i)}$ have been evaluated, any required properties of the wave field may be obtained. In particular, the water surface elevation η at time $t=0$, the wave height H and the wave phase angle ψ are given, respectively, as:

$$\eta(t=0) = \frac{H_0}{2} \text{Re}(\phi) = \frac{H}{2} \cos \psi \quad (33)$$

$$H = H_0 |\phi| \quad (34)$$

$$\psi = \text{Arg}(\phi) \quad (35)$$

where $\text{Re}(\)$ denotes the real part and $\text{Arg}(\)$ denotes the argument. A three-dimensional plot of $\eta(t=0)$ is useful for obtaining a general view of the wave field at a particular instant, with no special significance attached to the instant chosen, $t=0$. The wave height H and the wave phase angle ψ associated with ϕ have been expressed as above by taking ϕ in the form:

$$\phi = \frac{H}{H_0} \exp(i\psi) \quad (36)$$

A diffraction coefficient K_d may be defined as the ratio of the wave height at any point in the interior of the harbour to the incident wave height. Bearing in mind Eq. 34, this is given in terms of the scattered potential as:

$$K_d(\mathbf{x}) = |\phi_s^{(i)}(\mathbf{x})| \quad (37)$$

Finally, the wave direction at any point is also of interest, provided that

this can be identified in a meaningful way. The definition of wave direction θ adopted by Isaacson and Qu (1989) is that direction, measured clockwise from the x -axis, which is orthogonal to the wave phase angle contours and corresponds to increasing values of ψ . This definition can be expressed as:

$$\theta = \arctan \left(\frac{\partial \psi / \partial y}{\partial \psi / \partial x} \right) \quad (38)$$

The use of such a definition is really only suitable for portions of a wave field which have readily identifiable directions. In particular, for a wave field made up of component wave trains travelling in different directions, the wave direction at a point is somewhat artificial and not particularly meaningful. Provided that the definition given by Eq. 38 is adopted, then information on wave direction derives directly and visually from plots of phase angle contours, and it then becomes redundant to plot the direction itself.

Estimation of transmission coefficient

The preceding formulation is based on the assumption that the transmission coefficient α is known for all portions of the boundary S , and an appropriate manner of estimating α is now considered. As mentioned earlier, portions of the harbour boundary which are fully absorbing may simply be omitted from S , while for portions of S along fully reflecting boundaries, we have simply $\alpha = 0$. At partially reflecting boundaries, α can be estimated on the basis of Eq. 15 provided that suitable values are assigned to the conventional reflection coefficient K_r , the associated phase angle β and the incident wave direction γ . However, this may be rather difficult, and the estimation of each of these three parameters is considered in turn.

Reflection coefficient, K_r . For a particular beach or wall, the reflection coefficient K_r depends on the incident wave height, period and direction, but for simplicity a constant specified value of K_r is assumed for a particular beach or wall and a particular wave frequency.

Reflection phase angle β . The reflection phase angle β is directly related to the location at which the numerical vertical boundary is placed in relation to the actual boundary which may be sloping and in order to avoid ambiguity, the vertical boundary used in the numerical model is located where the still water level intersects the actual boundary. For a particular beach or wall, the reflection phase angle β will also depend on the incident wave height, period and direction, although experimental work relating to normal reflection at beaches and walls has generally provided information on reflection coefficients but not the associated phase angles. However, numerical tests have indicated that the results are not particularly sensitive to the value of β so that a value of $\beta = 0$ is chosen here.

Incident wave direction γ . The choice of γ is complicated because the flow at any point on the boundary generally contains incident waves together with reflected waves from other parts of the boundary. As indicated earlier, there is consequently some difficulty in adopting an incident wave direction in a meaningful way. Even if such a direction is obtained, say on the basis of Eq. 38, it will not generally be known *a priori*.

The simplest approach, which may be used to provide an initial approximation to the solution, is to take $\gamma=0$. Taken together with the assumption that $\beta=0$, this gives from Eq. 15:

$$\left. \begin{aligned} \alpha_1 &= 0 \\ \alpha_2 &= \frac{1 - K_r}{1 + K_r} \end{aligned} \right\} \quad (39)$$

In order to obtain improved values of γ , the wave field arising from this first approximation may be used to obtain a wave direction θ at any point on the boundary on the basis of Eq. 38. This direction may then be combined with the orientation of the boundary itself to provide the corresponding value of γ .

$$\gamma = \pi - \chi + \theta \quad (40)$$

where χ is the angle the normal to the boundary makes with the x -axis. This suggests an iterative procedure in which an initial solution is first found and used to provide the wave direction θ at each point on the boundary, and thus, by Eq. 40, the angle γ . The transmission coefficient α can then be estimated and a revised solution then obtained for the wave field.

RESULTS

The numerical model described above has been applied to the fundamental case of a rectangular harbour which is indicated in Fig. 2. The harbour has a length of 300 m and a width of 300 m, with a gap width B of 50 m between a pair of symmetrical breakwaters. The harbour is subjected to a uni-directional incident wave train of a uniform unit wave height, a propagation direction orthogonal to the breakwater gap as indicated in Fig. 2, and a length $L=50$ m corresponding to a breakwater gap to wave length ratio $B/L=1$. The incident wave train corresponds, for example, to a uniform depth $d=20$ m and a wave period $T=5.7$ s. In the numerical model, a source segment length to wave length ratio of $1/20$ has been used.

The wave field within the harbour predicted by the present method for the case of fully absorbing boundaries and impermeable breakwaters is indicated in Fig. 3. Since the harbour boundaries are fully absorbing in this case, they are not represented in the numerical model so that only the matching bound-

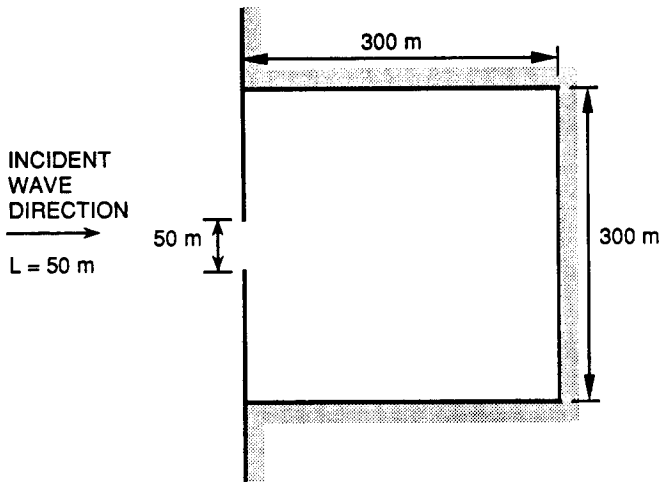


Fig. 2. Rectangular harbour used in numerical example.

ary across the breakwater gap is discretized. Note that the reflection coefficient along the breakwaters does not itself influence the solution in this particular case since the breakwaters are colinear with the gap, so that the wave sources along the gap do not induce a normal velocity along the breakwaters and reflections from elsewhere in the harbour are absent. More generally, for waves approaching the breakwater obliquely, the breakwater would have to be discretized and its reflection coefficient would then influence the solution. Figure 3a shows the computed water surface elevation at time $t=0$. This exhibits the expected features of wave crests which approximately form concentric arcs with centres at the breakwater gap, and wave heights which noticeably decrease in the shadow zone behind the breakwaters and which are close to the incident wave height outside the shadow zone. Figure 3b shows the corresponding contours of wave phase which reproduce this configuration of wave crests. Figure 3c shows the corresponding contours of wave height. These are compared to the predictions of the analytical solution (e.g. Blue and Johnson, 1949; Shore Protection Manual, 1984) shown in Fig. 3d, the numerical solution of Pos and Kilner (1987) shown in Fig. 3e which is based on a finite-element method, and the experimental measurements of Pos and Kilner (1987) shown in Fig. 3f. The comparison is quite favourable, with the general features of the analytical solution reproduced by the present numerical model.

In comparison to this case, Fig. 4 shows corresponding results for the identical conditions, except that the boundaries of the harbour are fully reflecting, $K_r=1$. This case of full reflection has been considered by Miles and Munk (1961), Garrett (1970) and Mei (1983) in the context of harbour resonance. However, a simple closed-form expression for the wave height within the harbour for arbitrary wave lengths is apparently not available. Figure 4a shows

the computed free surface elevation at time $t=0$ and indicates the generally confused, three-dimensional wave field within the harbour. Figures 4b and 4c show the corresponding wave phase and wave height contours, respectively, and clarify the irregularities of the wave field.

Figure 5 shows corresponding results for the more general case of boundaries with partial reflection corresponding to a reflection coefficient $K_r=0.1$. These results are based on the assumption that $\beta=0^\circ$ and $\gamma=0^\circ$. For the rel-

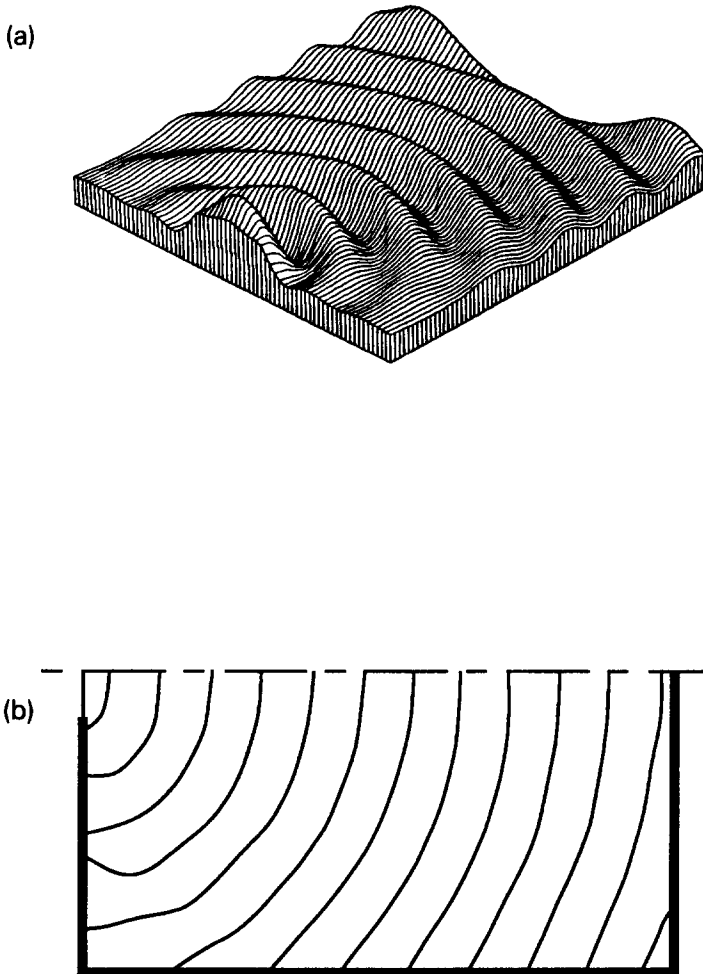
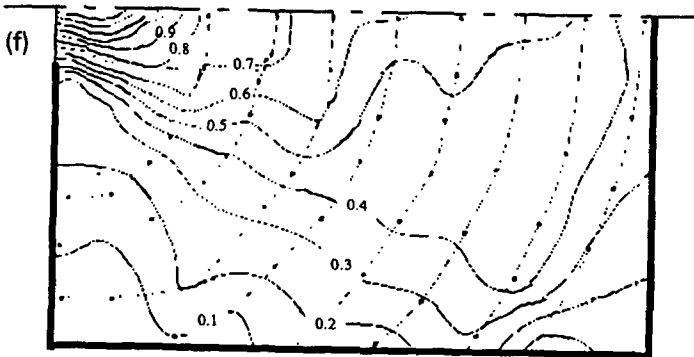
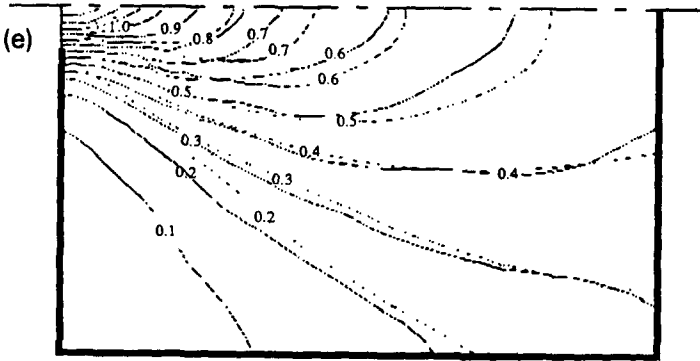
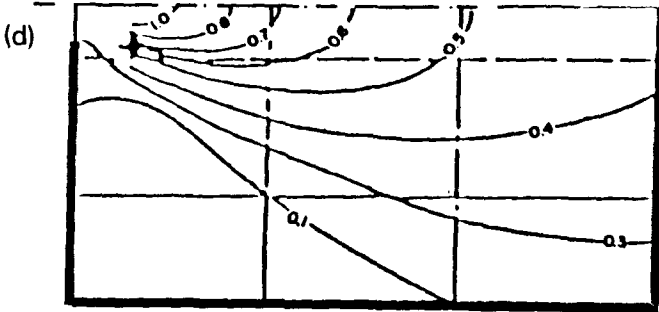
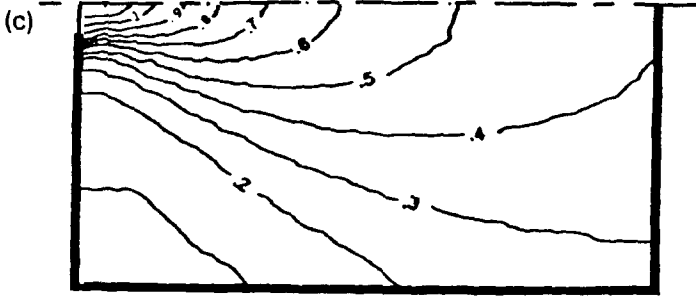


Fig. 3. Wave field in the rectangular harbour with fully absorbing boundaries. a, Surface elevation at time $t=0$; b, wave phase contours; c, wave height contours – present solution; d, wave height contours – analytical (Shore Protection Manual, 1984); e, wave height contours – numerical (Pos and Kilner, 1987); f, wave height contours – experiment (Pos and Kilner, 1987).



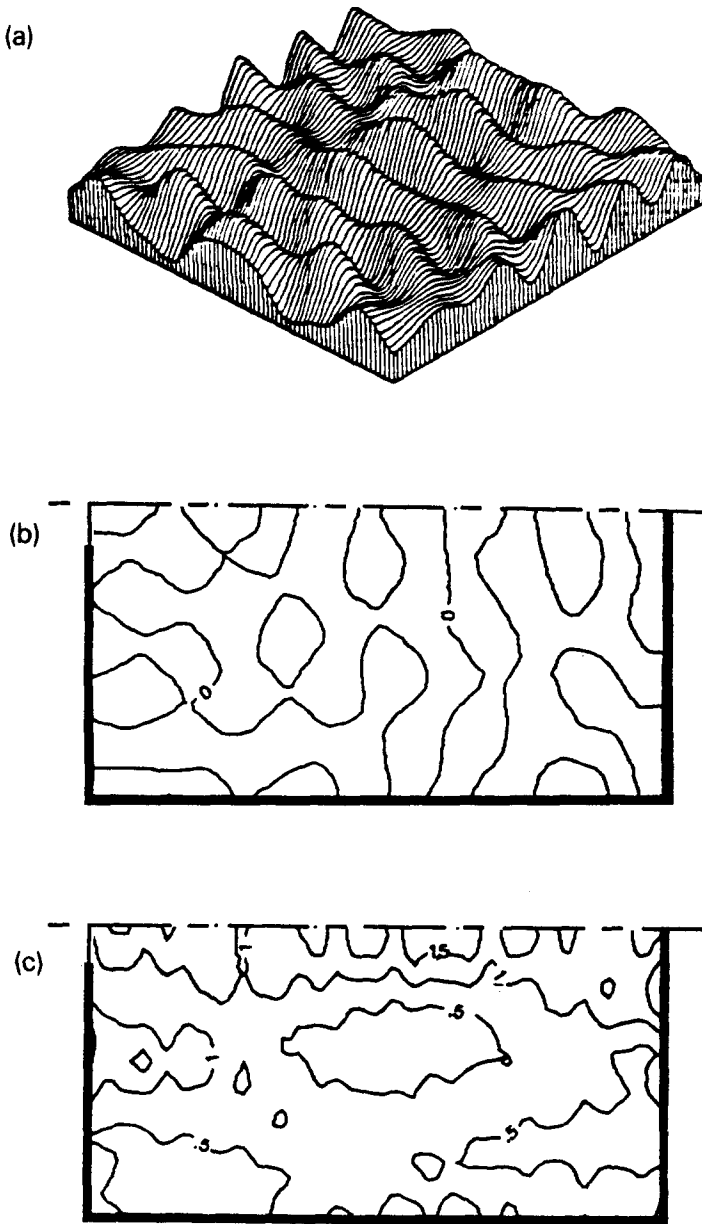


Fig. 4. Wave field in the rectangular harbour with fully reflecting boundaries. a, Surface elevation at time $t=0$; b, wave phase contours; c, wave height contours.

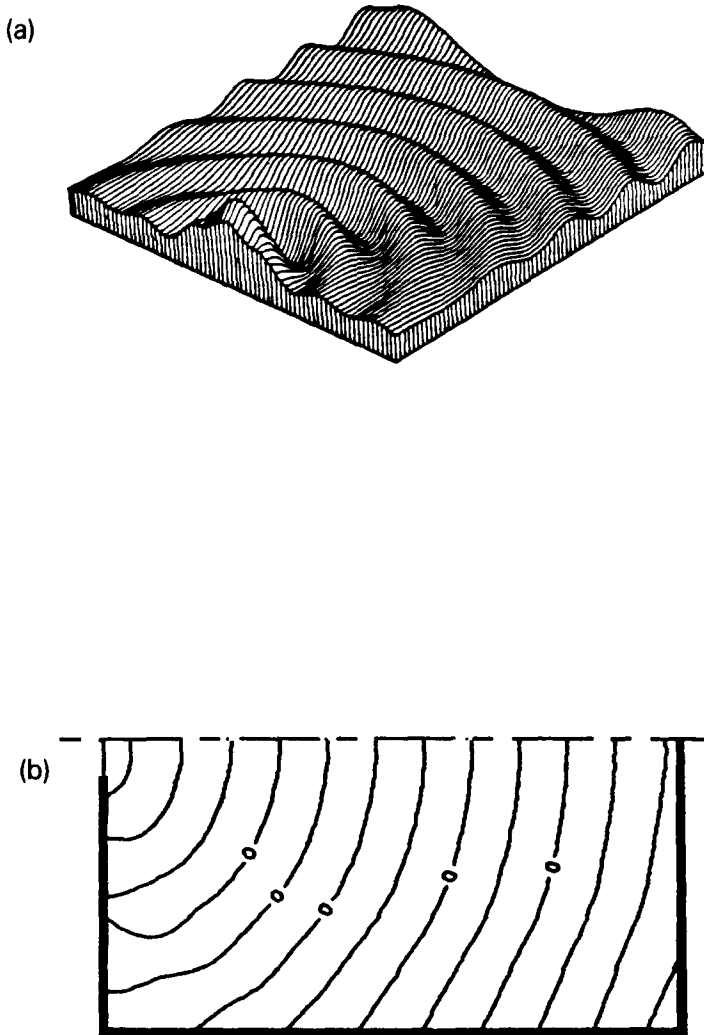


Fig. 5. Wave field in the rectangular harbour with partially reflecting boundaries: $K_r=0.1$, $\beta=0^\circ$, $\gamma=0^\circ$. a, Surface elevation at time $t=0$; b, wave phase contours.

atively low value of reflection coefficient adopted here, the results are not too different from the case of fully absorbing boundaries already indicated in Fig. 3. The water surface elevation at time $t=0$ and wave phase contours are shown in Figs. 5a and 5b, respectively, and exhibit no significant differences from the corresponding results for fully absorbing boundaries (indicated in Fig. 3a and 3b, respectively).

The wave height contours are more sensitive to the choice of reflection

coefficient and the trend due to an increasing reflection coefficient is now considered. Figure 6 compares the wave height contours for the example problem being considered, but with the reflection coefficient along the har-

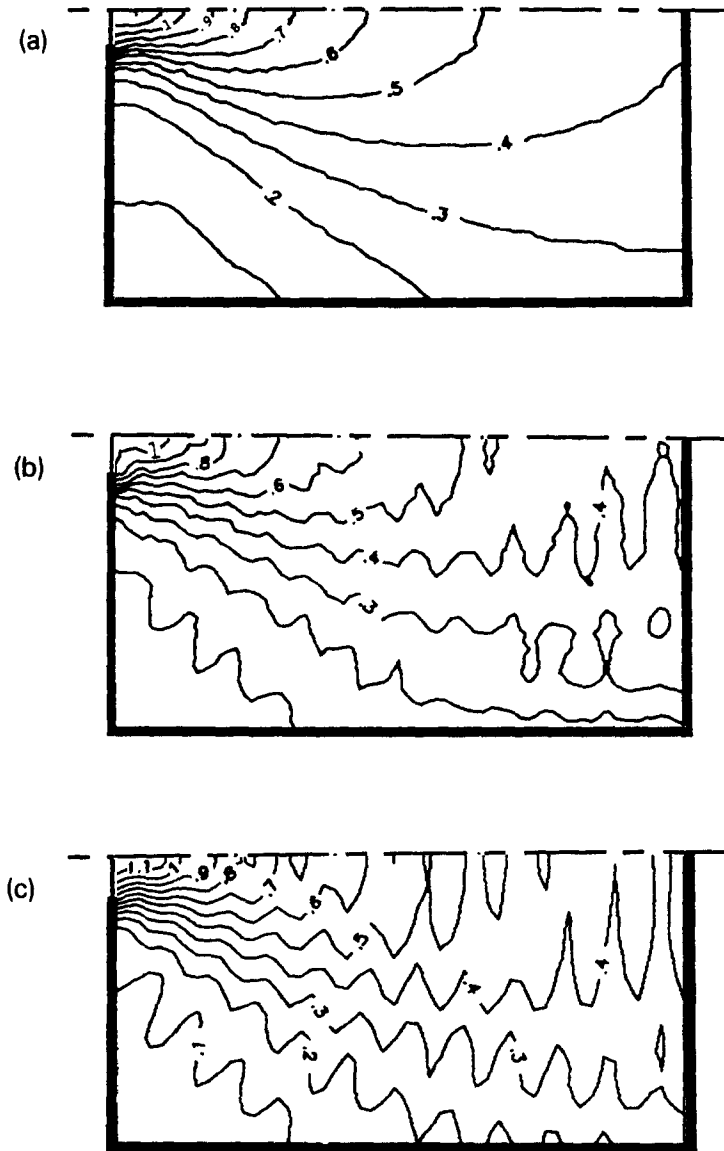


Fig. 6. Wave height contours in the rectangular harbour showing the effects of partial reflection. a, $K_r = 0$; b, $K_r = 0.1$; c, $K_r = 0.2$.

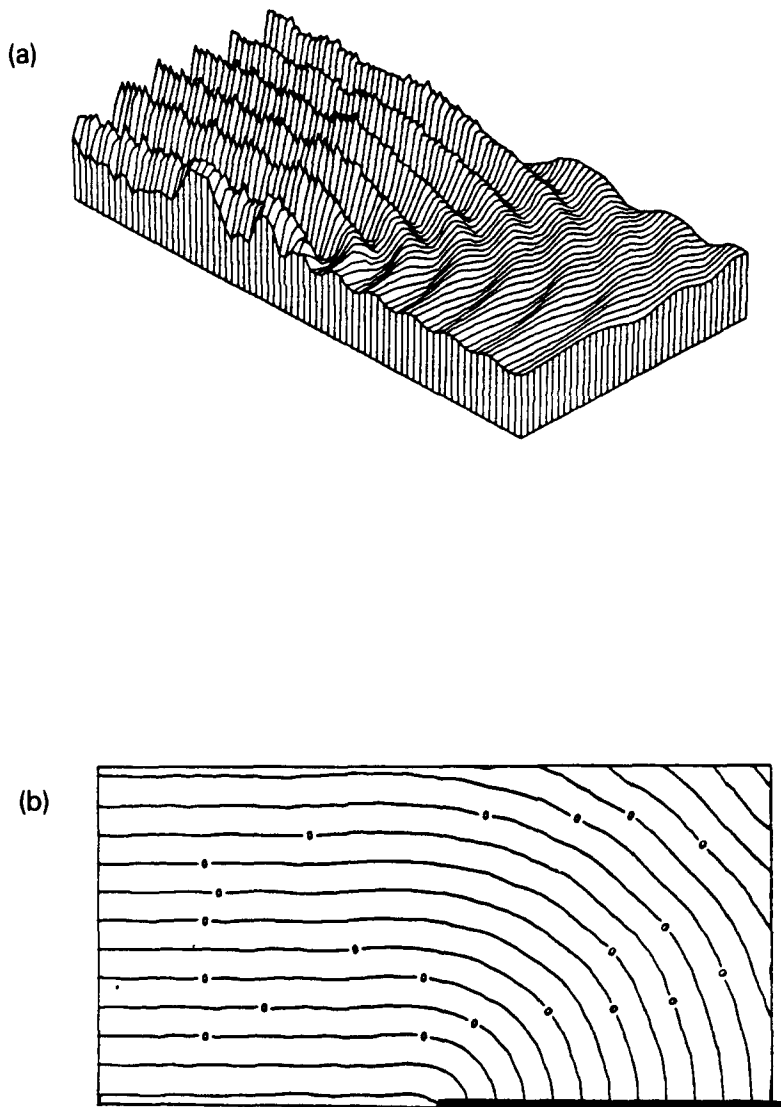


Fig. 7. Wave field behind a semi-infinite breakwater with fully absorbing boundaries. a, Surface elevation at time $t=0$; b, wave phase contours.

bour boundaries taken as $K_r=0, 0.1$ and 0.2 in turn. The figure shows an increasing irregularity in the wave height contours as a transition to the more confused state of full reflection, indicated in Fig. 4c, is being approached. This trend may explain the irregularities of the wave height contours measured by Pos and Kilner (1987) and shown in Fig. 3f in comparison to the smooth contours of the theoretical solution with no reflection shown in Fig. 3d.

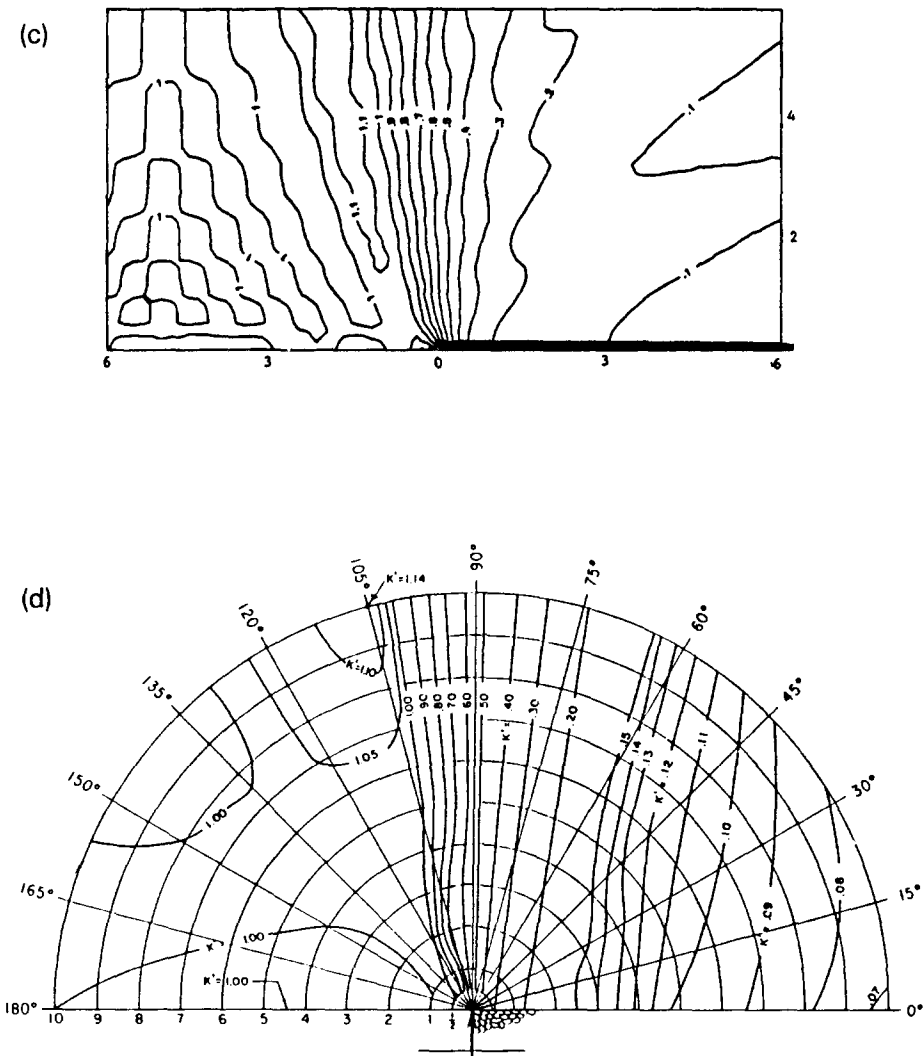


Fig. 7 (continued). Wave field behind a semi-infinite breakwater with fully absorbing boundaries. c, wave height contours – present solution; d, wave height contours – analytical (Shore Protection Manual, 1984).

The above results for partial reflection have all been obtained with $\beta=0^\circ$ and $\gamma=0^\circ$. Corresponding results for the same values of reflection coefficient K_r but with other values of β and γ have also been obtained. However, the general form of the wave field has been found not to be particularly sensitive to the values of β and γ selected, although some irregularities in the contours appear when γ is obtained by the iteration procedure described previously.

Finally, the present numerical model has been used to provide results for

the fundamental case of a semi-infinite breakwater with an incident wave train directed normal to the breakwater, for which an analytical solution is readily available (e.g. Shore Protection Manual, 1984). In the present numerical model, the matching boundary Γ was taken to have a length of 10 wave lengths extending from the breakwater tip, so that the case of a pair of colinear semi-infinite breakwaters with a breakwater gap to wave length ratio $B/L=10$ is actually modeled. For this particular set of results a source segment length equal to $L/10$, corresponding to 100 sources, was used.

Figure 7 shows the wave field in the vicinity of the breakwater. The computed water surface elevation at time $t=0$ and the corresponding contours of wave phase are shown in Fig. 7a and 7b, respectively. The figures exhibit the general features which are expected: within the shadow zone of the breakwater the wave crests form concentric arcs whose centre is at the breakwater tip, while outside the shadow zone the wave crests are straight. Figure 7c shows the corresponding contours of wave height which are compared to the predictions of the analytical solution shown in Fig. 7d. The agreement is generally quite favourable with the general features of the analytical model being reproduced by the numerical model. One feature of the numerical results which is not given by the analytical solution is that the contours of smaller wave heights exhibit an oscillatory variation not predicted by the analytical solution. In fact these are not unexpected and are also given by the analytical solution for the finite gap width $B/L=10$ which is actually being modeled.

Experimental measurements are needed to provide a more quantitative validation of the numerical model for the case of partially reflecting boundaries. For the present, though, it appears that the model predicts the wave field within the harbour realistically.

CONCLUSIONS

A numerical method has been developed to predict the wave field produced within a harbour of constant depth and arbitrary shape which contains partially reflecting boundaries. The approach used is based on linear diffraction theory and utilizes a point source representation of the harbour boundaries and a matching boundary at the harbour entrance. The boundary condition at a partially reflecting boundary involves a complex transmission coefficient which may be estimated from the conventional reflection coefficient K_r , a reflection phase angle β , and an incident wave direction γ .

Numerical results are presented for the wave field due to a specified incident wave train approaching a rectangular harbour with a pair of symmetrical breakwaters. Cases which are considered include perfectly absorbing, perfectly reflecting and partially reflecting harbour boundaries. In all these cases the numerical solution appears to predict the wave field within the harbour realistically. For cases of partial reflection, the effect of changes to the reflec-

tion parameters β and γ on the numerical solution has not been presented but it has been found that their choice does not influence the solution strongly.

REFERENCES

- Berkhoff, J.C.W., 1976. Mathematical models for simple harmonic water wave diffraction and refraction. Delft Hydraulics Lab., Rep. 168.
- Blue, F.L. and Johnson, J.W., 1949. Diffraction of water waves passing through a breakwater gap. *Trans. Am. Geophys. Union*, 30(5): 705-718.
- Chen, H.S., 1986. Effects of bottom friction and boundary absorption on water wave scattering. *Appl. Ocean Res.*, 8(2): 99-104.
- Chen, H.S. and Mei, C.C., 1974. Oscillations and wave forces in a man-made harbour in the open sea. *Proc. 10th Symp. Naval Hydrodynamics, Cambridge, Mass.*, pp. 573-596.
- Garrett, C.J.C., 1970. Bottomless harbours. *J. Fluid Mech.*, 43: 432-449.
- Hwang, L.-S. and Tuck, E.O., 1970. On the oscillations of harbours of arbitrary shape. *J. Fluid Mech.*, 42: 447-464.
- Isaacson, M. and Qu, S.-Q., 1989. Wave field due to a segmented generator and partially reflecting walls. *Coastal/Ocean Eng. Rep.*, Dep. Civil Eng., Univ. British Columbia, Vancouver, B.C.
- Mei, C.C., 1983. *The Applied Dynamics of Ocean Surface Waves*. Wiley, New York, N.Y., 740 pp.
- Miles, J.W. and Munk, W.H., 1961. Harbour paradox. *A.S.C.E. J. Waterw. Harbours Div.*, 87: 111-130.
- Pos, J.D. and Kilner, F.A., 1987. Breakwater gap wave diffraction: an experimental and numerical study. *A.S.C.E. J. Waterw. Harbours, Coastal Ocean Eng.*, 113(1): 1-21.
- Shore Protection Manual, 1984. Coastal Engineering Research Center, U.S. Army Corps of Engineers, Vicksburg, Miss.